Forest Ecology and Management 313 (2014) 69–82

Contents lists available at ScienceDirect

Forest Ecology and Management

journal homepage: www.elsevier.com/locate/foreco

# 3-PG simulations of young ponderosa pine plantations under varied management intensity: Why do they grow so differently?

Liang Wei [a,*], John D. Marshall [a,b], Jianwei Zhang [c], Hang Zhou [d], Robert F. Powers [c,†]

[a] Department of Forest, Rangeland, and Fire Sciences, University of Idaho, Moscow, ID 83844, USA
[b] Department of Forest Ecology and Management, Swedish Agricultural University, 901 83 Umeå, Sweden
[c] Pacific Southwest Research Station, USDA Forest Service, 3644 Avtech Parkway, Redding, CA 96002, USA
[d] Department of Geography, University of Idaho, Moscow, ID 83844, USA

ARTICLE INFO

*Article history:*
Received 25 September 2013
Accepted 22 October 2013
Available online 28 November 2013

*Keywords:*
Stable carbon isotope ratio
Quantum yield
Model calibration
Shrub competition
Canopy closure
Tree-ring

ABSTRACT

Models can be powerful tools for estimating forest productivity and guiding forest management, but their credibility and complexity are often at issue for forest managers. We parameterized a process-based forest growth model, 3-PG (Physiological Principles Predicting Growth), to simulate growth of ponderosa pine (*Pinus ponderosa*) plantations in Northern California. We used data collected from the "Garden of Eden" study, which was established in the 1980s to determine the effect of silvicultural treatments on plantation growth. We picked three sites representing a gradient of water availability and site productivity to run 3-PG. We modified the original linear canopy closure function to a power curve to capture observed stand dynamics *in situ*. We also added new functions to estimate the leaf area index and transpiration of the trees' understory competitors. These new functions restricted shrub growth with light intensity and assumed a fix ratio of shrub/tree transpiration per leaf area index. A $\delta^{13}C$ submodel, which estimated the ratio of stable carbon isotopes ($\delta^{13}C$) in plant tissue, played a key role in assigning values to gas-exchange parameters in the model. The resulting parameter values were similar to those fitted using sap flux. We replaced the original age modifier with tree-height based functions to reflect the decreased forest productivity as trees grew taller; tree height drove the change of maximum canopy conductance and its responsiveness to water vapor pressure deficit in the new functions. Some key parameters differed among sites, including quantum yield, maximum canopy conductance, and leaf allocation. The model successfully simulated the tree growth responses to fertilization and vegetation control at all three sites. The temporal variation of simulated shrub leaf area index was similar to the observed variation in shrub cover. These results help us to understand forest-growth responses to fertilizer and vegetation control, identify key tree and site parameters, and provide tuned model parameterizations that can predict the results of management alternatives in a changing climate.

© 2013 Elsevier B.V. All rights reserved.

## 1. Introduction

Forest process-based models (PBMs) are powerful tools assisting forest management (Korzukhin et al., 1996; Battaglia and Sands, 1998; Mäkelä et al., 2000; Johnsen et al., 2001). They incorporate components describing biophysical, ecological, and physiological processes of forests, which enables them to use environmental factors as model drivers and predict the impacts on forest growth in a changing world. This merit of PBMs is that they can help forest managers to cope with current climate change and the impacts of novel management scenarios (Korzukhin et al., 1996; Mäkelä et al., 2000).

A simple PBM, 3-PG (Physiological Principles Predicting Growth), is such a tool, designed to bridge the gap between the understanding of physiological processes and empirical forest mensuration data (Sands and Landsberg, 2002). It has been successfully applied to forest plantations all over the world (see a detailed review in Landsberg and Sands, 2011). The uses of 3-PG on plantations, as summarized by Almeida et al. (2004), are threefold: (1) estimating potential productivity for currently planted or future plantations; (2) analyzing factors that impact plantation growth; and (3) strategic planning on long-term wood supply. Our focus in this modeling project was to estimate the productivity of young ponderosa pine (*Pinus ponderosa* Lawson & C. Lawson) plantations with or without intensive management regimes, including fertilization and understory control.

Ponderosa pine is one of the most widely distributed pines in the western USA (Oliver and Ryker, 1990) and also the most widely planted tree species in northern California (Powers and Ferrell, 1996). Previous observations revealed that plantation growth was strongly correlated to available soil water and nutrients and that controlling competing vegetation significantly enhanced

* Corresponding author. Tel.: +1 208 301 0415.
*E-mail address:* liangwei@vandals.uidaho.edu (L. Wei).
† Deceased November 1, 2013.

0378-1127/$ - see front matter © 2013 Elsevier B.V. All rights reserved.
http://dx.doi.org/10.1016/j.foreco.2013.10.035

plantation growth (Powers and Ferrell, 1996; Powers and Reynolds, 1999). However, these trends had not been rigorously tested in experimentally designed studies across a gradient of site quality. Therefore, the "Garden of Eden" (GOE) study was established in the 1980s to determine how growth could be improved silviculturally and to develop a flexible model to predict growth response to competition control and fertilization (Powers et al., 1992).

Plots of the GOE study were installed with a common design at eight sites across northern California that covered varied geomorphic provinces and ranged from timbered land to brushfields (Powers and Ferrell, 1996). Silvicultural treatments included fertilizer, herbicide, and insecticide. The insecticide treatment was excluded in this study because there were no insect outbreaks at these sites during these years (Powers et al., 1992; Powers and Ferrell, 1996); however, the fertilizer and herbicide treatments significantly improved ponderosa pine growth (Powers et al., 1992; Powers and Ferrell, 1996; Powers and Reynolds, 1999; McFarlane et al., 2009; Zhang et al., 2013).

Since establishment of the GOE study, stand growth and development have been tracked for about 20 years. The detailed data provide an excellent opportunity to parameterize 3-PG for young ponderosa pine plantations across a range of treatments and site qualities. Earlier studies have applied 3-PG to natural ponderosa pine stands in Oregon, USA (Law et al., 2000, 2001; Coops and Waring, 2001; Coops et al., 2005). Aside from different geography, these studies focused on ecological and physiological questions; so they did not test their simulations with forest inventory data. This limited us from directly applying their parameterizations to the GOE plantations in northern California. We also faced the challenge of simulating forest dynamics with a significant shrub understory. Because 3-PG was designed for single-species stands (Landsberg and Waring, 1997), inter-specific competition from understory vegetation could not be estimated with the original formulation. Aggressive shrub species are ubiquitous in both natural stands and plantations of ponderosa pine in California. Therefore, shrub growth and water consumption must be considered.

Besides the understory submodel, model parameterization benefited from a new stable carbon isotope ($\delta^{13}C$) submodel (Wei et al., 2014). The $\delta^{13}C$ submodel simulated $\delta^{13}C$ in new photosynthate and tree-rings based on the existing description of carbon assimilation and canopy conductance in 3-PG. The simulations of $\delta^{13}C$ were sensitive to key parameters controlling carbon assimilation and canopy conductance, and hence errors in these parameters could be detected by comparing simulated $\delta^{13}C$ to observations (Wei et al., 2014). Because forest productivity, stomatal conductance, and transpiration varied among sites and treatments in the GOE study (Powers et al., 1992; Powers and Ferrell, 1996; Reynolds et al., 2000), some parameters are presumably different across sites and treatments for simulating carbon assimilation and canopy conductance. The $\delta^{13}C$ submodel could be valuable by facilitating parameterization and providing tests for the parameter values across sites and treatments.

The objectives of this modeling project included: (1) extending 3-PG to simulate the effects of fertilization and competition control on ponderosa pine growth while keeping the structure as simple as possible; (2) parameterizing 3-PG for young ponderosa pine plantations at GOE sites based on detailed field measurements; and (3) testing the $\delta^{13}C$ submodel for young stands.

## 2. Methods

### 2.1. Site description

Ponderosa pines were planted at eight locations in northern California in 1986–1988. Seedlings were raised in a common nursery before transplanting, and the best seed sources or families suitable to each specific site were used. The study was a completely randomized design with three replications at each site. Plot size was 19.5 × 21.9 m. Factorial combinations of herbicide (H), fertilizer (F), and insecticide application, each with two levels (with or without) yielded eight combinations in total. Treatments were randomly assigned to 24 plots in each site (Powers and Ferrell, 1996). Herbicide and insecticide were applied annually for the first six years; fertilizers were applied biennially (Powers and Reynolds, 1999). The formulations of fertilization were controlled at a rate to provide optimal nutrition for an average stand during its exponential phase of growth (Powers and Ferrell, 1996). Because there has been no insect outbreak since the test was established, no insecticide effect was found. We hence focused on four treatments in this modeling study, including control (C), fertilizer (F), herbicide (H), and H × F (HF).

Three GOE sites were chosen for this analysis (Table 1). Feather Falls (FF) represented the highest productivity and Elkhorn (EH) represented the lowest among all eight GOE sites; Whitmore (WH) represented the intermediate productivity (Powers and Ferrell, 1996). Climate at all sites was classified as Mediterranean, with wet winter and dry summer, but these sites also represented a temperature and moisture gradient. WH was the warmest followed by site FF and then EH. FF was the wettest and EH was the driest based on precipitation. The daytime vapor pressure deficit (VPD) was highest at WH and lowest at EH (Table 1, Fig. 1). The soil series were Sheetiron (loamy-skeletal, mesic Typic Dystroxerepts) at EH, Aiken (clayey, mesic Xeric Haplohumults) at WH, and Cohasset (loamy, mesic Ultic Haploxeralfs) at FF (McFarlane et al., 2010; Powers and Reynolds, 1999). We parameterized 3-PG for four treatments at each of these three sites; in total there were 12 site × treatment combinations.

### 2.2. 3-PG

3-PG is fundamentally a light-use efficiency model. It estimates gross primary production (GPP, $P_G$) from absorbed photosynthetically active radiation (APAR, $\phi_{pa}$, mol m$^{-2}$) and canopy light use efficiency ($\alpha_c$) (Landsberg and Waring, 1997). Environmental

**Table 1**
Properties of study sites. Site index (SI) was the average dominant tree height at year 50. SI at Whitmore was estimated from soil type and general climate because no suitable trees were available (Powers and Ferrell, 1996). *Sources:* †Powers and Ferrell (1996) and ‡McFarlane et al. (2010).

| Site | Coordinates | Elevation (m)† | SI (m)† | Annual precipitation (mm)† | Mean 2006 temperature (°C) | Plant year† | Previous vegetation† | Soil clay content‡ | Soil sand content‡ |
|---|---|---|---|---|---|---|---|---|---|
| Elkhorn (EH) | 40.05°N, −122.44°W | 1545 | 17 | 561 | 10.6 | 1988 | Plantation | 18 | 50 |
| Whitmore (WH) | 40.38 N, −121.541 W | 756 | 23 | 1016 | 14.5 | 1986 | Brushfield | 31 | 42 |
| Feather Falls (FF) | 39.37 N, −121.12 W | 1246 | 30 | 1308 | 11.7 | 1988 | Natural stand | 27 | 41 |

factors reduce the light-use efficiency from the canopy-scale quantum yield ($\alpha_{cx}$, mol C mol$^{-1}$ photon), which is the maximum light use efficiency restricted only by physiological processes. GPP (mol m$^{-2}$) is then estimated as (Sands and Landsberg, 2002; Landsberg and Sands, 2011):

$$P_G = \alpha_c \phi_{pa} = \alpha_{cx} \varphi f_T f_F f_N \phi_{pa} \quad (1)$$

where $f_T$, $f_F$ and $f_N$ are the modifiers for temperature, frost, and fertility respectively. Equations for all the modifiers can be found in Sands and Landsberg (2002) and Wei et al. (2014). $\varphi$ is a modifier describing the effects of water status as:

$$\varphi = f_{VPD} f_{SW} \quad (2)$$

where $f_{VPD}$ and $f_{SW}$ are the modifiers for VPD (mBar, 1 mBar = 0.1 kPa) and soil water respectively. We made two changes in these equations from their original form, which was described as min($f_{VPD}$,$f_{SW}$)$f_{age}$, where $f_{age}$ is an age modifier (Landsberg and Waring, 1997). We first removed $f_{age}$ and used tree-height based equations to estimate the change of forest productivity and canopy conductance with tree height (see Section 2.3). Secondly, we used the Jarvis (1976)-form equation, $f_{VPD} \times f_{SW}$, instead of min($f_{VPD}$, $f_{SW}$). Communication between us and the original 3-PG authors (Richard Waring, Peter Sands, and Joe Landsberg) encouraged us to make this modification. Moreover, when 3-PG was coupled with a $\delta^{13}$C submodel (see Section 2.3), this Jarvis-form of $\varphi$ improved the simulations of tree ring $\delta^{13}$C; $R^2$ between simulations and observations increased by 0.08 based on the data of Wei et al. (2014), which used the old equation (unpublished data).

Otherwise, the model behaves as described previously. In Eq. (2), $f_{VPD}$ is a function of water VPD ($V$):

$$f_{VPD} = \exp(-k_g \times V) \quad (3)$$

where $k_g$ (mBar$^{-1}$; 1 mBar = 0.1 kPa) is a constant (Landsberg and Waring, 1997). We assumed that one mol of carbon was equal to 24 g dry biomass and converted the units of GPP to Mg biomass ha$^{-1}$ yr$^{-1}$.

The current version of the model estimates APAR from the solar radiation input (MJ m$^{-2}$):

$$\phi_{pa} = 4.6 p_s \phi_s c (1 - e^{-kL}) \quad (4)$$

where 4.6 converts the units of radiation from MJ m$^{-2}$ to mol m$^{-2}$ as 1 MJ PAR ≈ 4.6 mol quanta PAR (PAR = photosynthetically active radiation); $p_s$ is a factor describing the proportion of energy of solar radiation that lies in the PAR spectrum (400–700 nm); $c$ is a factor describing the proportional canopy closure during stand development (see Section 2.5 below); $k$ is the extinction coefficient for absorption of PAR by canopy (0.52, Pierce and Running, 1988); and $L$ is the leaf area index (LAI, m$^2$ leaf m$^{-2}$ ground area). We set $p_s$ to 0.56 as indicated from measurements of two study sites (see Section 2.7). Beer's Law was embedded in this function to describe the proportion of solar radiation transmitted through the canopy ($p_L$) as:

$$p_L = e^{-kL} \quad (5)$$

Net primary production (NPP, Mg ha$^{-1}$) was assumed a fixed ratio of GPP (Landsberg and Waring, 1997; Waring et al., 1998); we used NPP/GPP = 0.45 for ponderosa pine (Law et al., 1999). NPP was then allocated among stem (branch + trunk), foliage, and root. The allocation to roots is determined by soil fertility and growing conditions (i.e. $\varphi$ in Eq. (2)) (Landsberg and Waring, 1997; Sands and Landsberg, 2002). The remainder carbon is then allocated between stem and foliage using a DBH-related function (Sands and Landsberg, 2002).

3-PG also describes a simple water balance. It considers the soil as a container with the maximum volume set as maximum available water-holding capacity (i.e., *maximum available soil water* in 3-PG); the instantaneous volume of water pool, available soil water (ASW), was determined by water balance. Inputs to the soil water pool are precipitation and irrigation. Excess water leaves the system as runoff. Water is also removed from the soil pool by evapotranspiration, which is estimated by the Penman–Monteith equation.The canopy conductance ($g_c$, m s$^{-1}$) to water vapor is estimated as a function of water status (Landsberg and Waring, 1997; Sands, 2001):

$$g_c = g_{cmax} \varphi \min(1, L/L_x) \quad (6)$$

where $L_x$ is the LAI value at which canopy conductance attains its maximum value, and $g_{cmax}$ is the maximum canopy conductance. In this study, we changed $g_{cmax}$ with stand tree height.

### 2.3. Impacts of tree height

As trees gain height, they face more difficulty transporting water to the canopy. As a consequence, both stomatal conductance and photosynthesis are reduced (Ryan and Yoder, 1997; Hubbard et al., 1999; McDowell et al., 2002; Koch et al., 2004). Height is hence the main driver of what were considered "age"-effects in the original 3-PG formulation. Moreover, if we used the $f_{age}$ in the original 3-PG to consider such "age"-effects, as forest productivity varied dramatically across treatments and sites in this study, the $f_{age}$ had to be specifically adjusted for every treatment. We hence removed the original $f_{age}$ and used two new equations to relate the developmental changes of $g_{cmax}$ and $k_g$ to the true driver, tree height. We assumed that $g_{cmax}$ and $k_g$ decreased linearly with tree height as:

$$g_{cmax} = g_{cmax0} + s_g H_t \quad (7)$$

$$k_g = k_{g0} + s_k H_t \quad (8)$$

where $k_{g0}$ is the $k_g$ of seedlings (mBar$^{-1}$), $H_t$ is the mean stand tree height (m), $g_{cmax0}$ is of the $g_{cmax}$ of seedlings (m s$^{-1}$), and $s_k$ (mBar$^{-1}$ m$^{-1}$) and $s_g$ (m s$^{-1}$ m$^{-1}$) are the change rates of $k_g$ and $g_{cmax}$ respectively with tree height. The response of canopy or stomatal conductance to VPD was measured from trees of two height classes for ponderosa pine. For ponderosa pine, in each of three studies (Hubbard et al., 1999; Ryan et al., 2000; Law et al., 2001), canopy or stomatal conductance was lower for taller trees at the same VPD, and canopy or stomatal conductance declined more steeply with VPD (i.e. larger $k_g$) in taller trees. We hence knew that $s_k$ was positive and $s_g$ was negative. We calibrated $s_k$ and $s_g$ at the fast-growing HF treatment of site FF and then applied them to other treatments and sites. $k_{g0}$ and $g_{cmax0}$ were fitted for each treatment by the aid of the $\delta^{13}$C submodel (see Section 2.9).

We embedded a DBH based allometric equation in 3-PG to estimate tree height as (Wykoff et al., 1982):

$$H_t = 0.3048\left(e^{\beta_0 + \beta_1/(D/2.54+1)} + 4.5\right) \quad (9)$$

where $H_t$ is the mean tree height of a stand (m), $\beta_0$ and $\beta_1$ are species-dependent constants, and $D$ is the mean stand DBH (cm). We fitted $\beta_0$ and $\beta_1$ based on the GOE data and found that $\beta_0$ = 0.0561 and $\beta_1$ = 2.488; this equation explained 93% of the variation and the simulated stand mean $H_t$ were not different from observations at the 0.05 level.

### 2.4. 3PG-$\delta^{13}$C

We modified 3-PG by extending it to calculate carbon stable isotope ratio ($\delta^{13}$C) of new photosynthate and tree rings (described

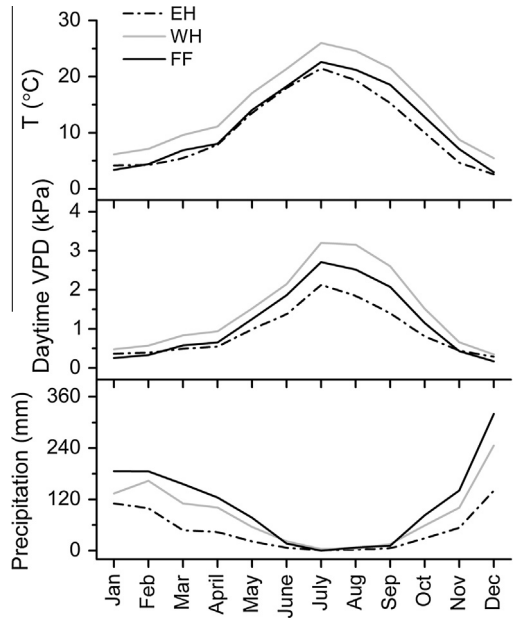


**Fig. 1.** Monthly mean temperature, mean daytime VPD, and total precipitation at three GOE sites. Data are multi-year averages of 3-PG inputs from 2001 to 2010.

in Wei et al. (2014)). The $\delta^{13}C$ of new photosynthate ($\delta^{13}C_p$) in a $C_3$ plant can be approximated as (Farquhar et al., 1982):

$$\delta^{13}C_p \approx \delta^{13}C_a - a - (b - a)(c_i/c_a) \tag{10}$$

where $\delta^{13}C_a$ is the isotopic composition of air, $a$ is the fractionation against $\delta^{13}C$ in diffusion (4.4‰), $b$ is an empirical coefficient determined mostly by the enzymatic fractionation of Rubisco (27 ‰), and $c_i$ and $c_a$ are leaf internal and ambient $CO_2$ concentrations, respectively. Parameter $c_i$ can be estimated based on the photosynthetic gas-exchange of plants as (Farquhar and Sharkey, 1982):

$$c_i = c_a - \frac{A}{g} \tag{11}$$

where $A$ is the $CO_2$ net assimilation rate in mol C $m^{-2}$ $s^{-1}$, and $g$ is the stomatal conductance to the diffusion of $CO_2$ (mol C $m^{-2}$ $s^{-1}$). 3-PG treats the canopy as a big leaf (Farquhar, 1989), so we estimated plant average $\delta^{13}C_p$ by combining Eqs. (10) and (11):

$$\delta^{13}C_p \approx \delta^{13}C_a - a - (b - a)\left(1 - \frac{A}{c_a g}\right) \tag{12}$$

$A$ was obtained from the GPP simulation of 3-PG by converting the units from Mg $ha^{-1}$ $month^{-1}$ to mol C $m^{-2}$ $s^{-1}$; and $g$ was calculated from outputs of canopy conductance to water vapor by converting units from m $s^{-1}$ to mol C $m^{-2}$ $s^{-1}$ and applying the ratio of diffusivities of $CO_2$ to water vapor in air (0.66, Campbell and Norman, 1998).

A constant offset ($\varepsilon_{sp}$) was assumed between $\delta^{13}C$ in new photosynthate and wood in the annual growth ring for this version of $\delta^{13}C$ submodel (see Wei et al., 2014 for the validation and limits). The monthly ring wood $\delta^{13}C$ ($\delta^{13}C_s$) was then estimated as:

$$\delta^{13}C_s = \delta^{13}C_p + \varepsilon_{sp} \tag{13}$$

The $\delta^{13}C$ of a whole ring was calculated as the mean $\delta^{13}C_s$ weighted by modeled monthly increment of stem mass over a whole growing season.

The second modification made in our earlier work on 3-PG was to add a linear temperature modifier (Uddling et al., 2005) to the calculation of canopy conductance (Wei et al., 2014):

$$f(T)_{gc} = \min(1, k_2 + k_3 T_{av}) \tag{14}$$

where $T_{av}$ is monthly mean air temperature and $k_2$ and $k_3$ are empirical constants (Table 2). This was necessary to restrict wintertime transpiration.

### 2.5. New function for canopy closure

In this study, we modified a function to improve the model's description of canopy light interception before canopy closure. The 3-PG model currently assumes that only a proportion of PAR, which is described by canopy cover, $c$, can be intercepted by the canopy before the age of canopy closure ($t_{cc}$). In the $t$th year ($t < t_{cc}$), intercepted PAR is proportional to $c = t/t_{cc}$. This linear function describes the light interception before the forming of the "big leaf" and restricts the early growth in the simulations. Field observations (Fig. 2) indicated that the annual growth of ponderosa pine crowns did not follow a linear pattern in most GOE treatments. We hence modified the canopy closure function of 3-PG to a power function as indicated from the field observations (Fig. 2):

$$c = \left(\frac{t}{t_{cc}}\right)^{n_{cc}} \tag{15}$$

where $n_{cc}$ is a constant. This function was tested with field observations and $t_{cc}$ was estimated (Fig. 2). The observed canopy cover was estimated from $c = A_c/4.7$, where $A_c$ is the mean crown area in $m^2$, as estimated for a circular crown, and, 4.7 $m^2$ is the average crown area when the crowns of adjacent trees first meet, as calculated from the known spacing of the planted trees. Data from H and HF treatments were first used to determine $n_{cc}$ because shrub competition delayed canopy expansion in the other plots (Shainsky and Radosevich, 1986). This delay was especially protracted on the C treatments at sites EH and WH (Fig. 2). For the control treatments at these sites, we have therefore retained the linear function by setting $n_{cc} = 1$ (Fig. 2).

### 2.6. Shrub competition

Woody shrubs are regarded as the strongest competitors of ponderosa pine (Reynolds et al., 2000). Presence of shrubs reduced tree growth at non-herbicide treatments (Shainsky and Radosevich, 1986; Powers and Reynolds, 1999) and delayed the timing of canopy closure (Fig. 2, Table 3). The dominant shrubs were mixed evergreen *Arctostaphylos* spp. and deciduous *Ceanothus* spp. at all sites (McFarlane et al., 2010).

To simulate the impact of shrub competition on tree growth, we needed to determine shrub growth dynamics and subsequently the interaction between shrubs and trees. Ponderosa pine and the shrubs may compete for three resources: nutrients, soil water, and light (Shainsky and Radosevich, 1986). With regard to nutrients, herbicide application had either nil or negative effect on the N pools at our sites; there were no changes in total N or C/N ratio in the upper 20 cm of mineral soil when comparing the C vs. H, and F vs. HF pairs; N concentration of soil was higher in the C than H treatment at EH (McFarlane et al., 2010). Although it is risky to infer nutrient availability from nutrient pool-size, these results lead us to suggest that understory presence did not deplete soil N and may have increased it. In any case, it seems that it should not be a major factor in simulating shrub and tree competition at our sites. With regard to water, Shainsky and Radosevich (1986) measured canopy conductance in mixtures and monocultures of *Arctostaphylos* and ponderosa pine seedlings with *Arctostaphylos*/pine stem proportions of 0/100, 25/75, 50/50, 75/25, and 100/0. They found that *Arctostaphylos* maintained constant stomatal conductance among treatments, but ponderosa pine in the mixtures could not maintain stomatal conductance as high as in the pine

**Table 2**
Values and sources of identical parameters across simulations. Notations follow Sands and Landsberg (2002). Data marked "observed" were obtained in former GOE studies; "fitted" data were calibrated in this study based on measured data; and "Default" data were set as default in $3PG_{PJS}$ model.

| Parameters | Symbols | Units | Values | Sources |
|---|---|---|---|---|
| *Biomass and volume estimation* | | | | |
| Foliage:stem partitioning ratio @ DBH = 2 cm | $p_2$ | – | 1 | Default |
| Constant in the stem mass vs. diameter relationship | $a_s$ | – | 0.0561 | Observed |
| Power in the stem mass vs. diameter relationship | $n_s$ | – | 2.488 | Observed |
| Minimum fraction of NPP to roots | $\eta_{Rn}$ | – | 0.25 | Default |
| Maximum fraction of NPP to roots | $\eta_{Rx}$ | – | 0.80 | Default |
| Ratio NPP/GPP | – | – | 0.45 | Law et al. (1999) |
| *Modifiers for photosynthesis* | | | | |
| Minimum temperature for growth | $T_{min}$ | °C | 0 | Law et al. (2000) |
| Optimum temperature for growth | $T_{opt}$ | °C | 20 | Law et al. (2000) |
| Maximum temperature for growth | $T_{max}$ | °C | 40 | Law et al. (2000) |
| Days production lost per frost day | $k_F$ | day | 1 | Default |
| *Litterfall and root turnover* | | | | |
| Maximum litterfall rate | $\gamma_{Fx}$ | $month^{-1}$ | 0.021 | Law et al. (2000) |
| Litterfall rate at $t = 0$ | $\gamma_{F0}$ | $month^{-1}$ | 0.001 | Default |
| Age at which litterfall rate has median value | $t_{\gamma F}$ | month | 36 | Coops et al. (2005) |
| Average monthly root turnover rate | $\gamma_R$ | $month^{-1}$ | 0.015 | Default |
| *Conductance* | | | | |
| LAI for maximum canopy conductance | $L_x$ | – | 3.3 | Default |
| Canopy boundary layer conductance | $g_B$ | $m\ s^{-1}$ | 0.2 | Default |
| *Stem mortality* | | | | |
| Power in self-thinning rule | $n_m$ | – | 1.5 | Default |
| Fraction single-tree foliage biomass lost per dead tree | $m_F$ | – | 0 | Default |
| Fraction single-tree root biomass lost per dead tree | $m_R$ | – | 0.2 | Default |
| Fraction single-tree stem biomass lost per dead tree | $m_S$ | – | 0.2 | Default |
| *Canopy structure and processes* | | | | |
| Specific leaf area at age 0 | $\sigma_0$ | $m^2\ kg^{-1}$ | 4.2 | Observed |
| Specific leaf area for mature leaves | $\sigma_1$ | $m^2\ kg^{-1}$ | 4.2 | Observed |
| Extinction coefficient for absorption of PAR by canopy | $k$ | – | 0.5 | Pierce and Running (1988) |
| Maximum proportion of rainfall evaporated from canopy | $I_x$ | – | 0.15 | Default |
| LAI for maximum rainfall interception | $L_{Ix}$ | – | 0 | Default |
| *New submodels* | | | | |
| Rate of $k_g$ change with tree height | $s_k$ | $mBar^{-1}\ m^{-1}$ | 0.001 | Fitted |
| Rate of $g_{cmax}$ change with tree height | $s_g$ | $m\ s^{-1}\ m^{-1}$ | −0.00016 | Fitted |
| Ratio of the per-LAI transpiration of the shrub/tree | $p_{ST}$ | – | 1 | Assumed (see Section 2.6) |
| Temperature modifier for $g_c$: $k_2$ | $k_2$ | – | 0.244 | Uddling et al. (2005) |
| Temperature modifier for $g_c$: $k_3$ | $k_3$ | – | 0.0368 | Uddling et al. (2005) |
| The ratio of diffusivities of $CO_2$ and water vapor in air | – | – | 0.66 | Farquhar et al. (1982) |
| $\delta^{13}C$ difference of tissue and new phophotosynthate | $\varepsilon_{sp}$ | ‰ | 1.7 | Fitted |
| Fractionation against $^{13}C$ in diffusion through air | $a$ | ‰ | 4.4 | Farquhar et al. (1982) |
| Enzymatic fractionation by Rubisco | $b$ | ‰ | 27 | Farquhar et al. (1982) |

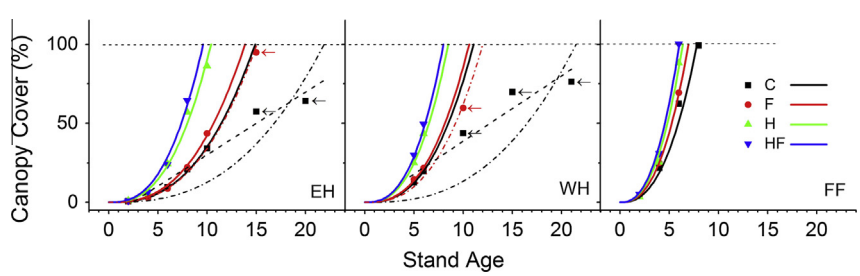


**Fig. 2.** The new canopy closure function for 3-PG. Dots are canopy cover estimates from average tree crown area divided by 4.7 $m^2$. Colored lines were fitted using new canopy closure model for four treatments (Eq. (15)): Control (C), Fertilizer (F), Herbicide (H), and H × F (HF). When a colored line intercepts the 100% line, the value on the *x*-axis is the canopy closure year ($t_{cc}$). For C and F treatments at site EH and WH, solid lines were fitted using dots before stand age 10 (visually determined), and points with arrows were not used; dash-dot lines were fitted with all points. The shrub competition may have slowed down the tree growth and hence the canopy-closing process at C and F treatments. We applied the parameters of the solid fitting lines to the 3-PG modeling, except the C treatments at site EH and WH. We used straight lines for C treatments at EH and WH ($n_{cc} = 1$, Eq. (15)) for there two treatments, and $t_{cc}$ was adjusted to fit the simulated volume to the observation at these two treatments.

monoculture. This indicated that the *Arctostaphylos* was a stronger competitor for soil water than the pine. With regard to light, trees were taller than shrubs starting no later than age four, and the heights of lower tree crown were either similar to or taller than shrub heights in most treatments – except the C treatments at EH and WH (unpublished data). The rapid emergence of trees through the shrub canopies allowed us to infer that light may have limited shrub growth. Therefore, we used light to describe the im-

pact of trees on shrub growth, then estimated water consumption by the shrubs to describe the impact of shrub competition on tree growth.

We modeled the competition for soil water by accounting for shrub transpiration as it draws from the soil water pool. To keep the structure simple, we assumed first that transpiration of the shrubs was proportional to shrub LAI/total LAI. Second, we assumed that LAI of shrubs ($L_S$) was related to tree LAI such that shrub LAI initially increases with tree LAI ($L$) and then deceases with tree LAI when light transmission through the tree canopy decreases.

Our approach estimated LAI of shrubs from LAI of trees. As indicated by field observations (comparing Figs. 2 and 3), the shrub cover generally increased after trees were planted and then decreased around the year of tree canopy closure. We hence defined two phases for shrub LAI estimation to simplify the simulation of shrub LAI, including a linear increase early in stand establishment and a negative exponential decrease when shrub growth was limited by light. In the linear stand-establishment phase, we assumed that light was not a limiting factor, so the shrub growth experienced the same limiting factors as trees did. We assumed that $L_S$ is a fixed ratio ($K_L$) of tree LAI in this phase. The function can be expressed as:

$$L_S = K_L L \tag{16}$$

After the phase of non-limiting light, light and other environmental factors limited shrub growth. The impact of environment was represented by a parameter that describes the theoretical maximum LAI that shrubs may reach if trees were absent and all resources were abundant (denoted $L_{SX}$). The light impact on shrub growth was then estimated as proportional to the amount of light passing through the tree canopy, which was estimated with Eq. (5) (Fig. 4b). We then created a function similar to Eq. (5) to estimate $L_S$ when light was limiting:

$$L_s = L_{SX} e^{-kL} \tag{17}$$

We defined that the shrub LAI passed the stand-establishment phase once the value using Eq. (16) was larger than the value of Eq. (17), which guaranteed a smooth transition between the two functions.

After $L_S$ was estimated, transpiration by shrubs ($T_S$) was estimated as:

$$T_S = \frac{T_T}{L} L_S p_{ST} \tag{18}$$

where $T_T$ is total transpiration of the trees estimated by 3-PG, and $p_{ST}$ is the ratio of the per-LAI transpiration of the shrub to the tree. This function assumes that the monthly shrub transpiration and tree transpiration are proportional, which was supported by the sap flow data in Fisher et al. (2007). In their study, sap flow was measured for ponderosa pine and two shrubs (*Arctostaphylos manzanita* and *Ceanothus cordulatus*) for one year in northern California. We reanalyzed their data and found a fixed $p_{ST}$: the monthly mean daily sap flux data ($P < 0.01$). However, we could not estimate $p_{ST}$ based on Fisher et al. (2007) because individual observations were not scaled up to stand level. For the present, we assumed $p_{ST} = 1$ in this study.

The new shrub LAI and transpiration functions avoid detailed descriptions of shrub growth and transpiration by adding only three new parameters to 3-PG. This approach is flexible as it al-

**Table 3**
Parameters that differed among sites or treatments. Three non-calibrated parameters were determined by measurements: quantum yields ($\alpha_{cx}$, mol C mol$^{-1}$ photon), initial stocking (trees ha$^{-1}$), and wood density (g cm$^3$). Parameters $t_{cc}$ (year, rounding down) and $n_{cc}$ (unitless) were fitted with observed canopy area data (Eq. (15)). Other site/treatment different parameters are: maximum available soil water ($ASW_{max}$, mm), fertility rating, maximum shrub LAI that free growing shrubs can reach ($L_{SX}$, m$^2$ m$^{-2}$), the ratio of shrub/tree LAI at stand establishment ($K_L$), maximum canopy conductance of seedlings ($g_{cmax0}$, m s$^{-1}$), constant for stomatal response to VPD of seedlings ($k_{g0}$, mBar$^{-1}$), allocation to foliage when DBH = 20 cm ($p_{20}$), and branch and bark fraction for young stand (age = 0, $p_{B0}$) and mature stands ($p_{B1}$) (Sands and Landsberg, 2002). Underlined numbers were calibrated in 3-PG by fitting simulations to observations.

| Sites | EH | | | | WH | | | | FF | | | |
|---|---|---|---|---|---|---|---|---|---|---|---|---|
| Treatments | C | F | H | HF | C | F | H | HF | C | F | H | HF |
| $\alpha_{cx}$ (SE) | 0.056 (0.003) | | | | 0.049 (0.003) | | | | 0.048 (0.004) | | | |
| Initial stocking | 1374 | 1065 | 1374 | 1290 | 1402 | 1290 | 1682 | 1626 | 1682 | 1682 | 1682 | 1654 |
| Wood density | 0.41 | 0.39 | 0.39 | 0.39 | 0.39 | 0.36 | 0.36 | 0.36 | 0.35 | 0.30 | 0.33 | 0.30 |
| $n_{cc}$ | 1 | 2.6 | 2.6 | 2.6 | 1 | 2.6 | 2.6 | 2.6 | 2.6 | | | |
| $t_{cc}$ | 24 | 14 | 10 | 9 | 11 | 10 | 8 | 8 | 7 | 6 | 6 | 6 |
| $ASW_{max}$ | 130 | | | | 130 | | | | 1000 | | | |
| Fertility rating | 0.6 | 1.0 | 0.6 | 1.0 | 0.5 | 1.0 | 0.6 | 1.0 | 0.5 | 1.0 | 0.5 | 1.0 |
| $L_{SX}$ | 0.9 | 1.8 | – | – | 4.6 | 8.6 | – | – | 12.0 | 19.0 | – | – |
| $K_L$ | 1 | 1 | 0 | 0 | 1 | 1 | 0 | 0 | 1 | 1 | 0 | 0 |
| $g_{cmax0}$ | 0.011 | 0.013 | 0.013 | 0.014 | 0.009 | 0.008 | 0.008 | 0.008 | 0.009 | 0.011 | 0.011 | 0.011 |
| $k_{g0}$ | 0.085 | 0.085 | 0.078 | 0.072 | 0.062 | 0.044 | 0.027 | 0.025 | 0.023 | 0.019 | 0.023 | 0.022 |
| $p_{20}$ | 0.10 | 0.15 | 0.16 | 0.24 | 0.16 | 0.20 | 0.21 | 0.24 | 0.18 | 0.22 | 0.21 | 0.22 |
| $p_{B0}$ and $p_{B1}$ | 0.3 | | | | 0.26 | | | | 0.35 | | | |

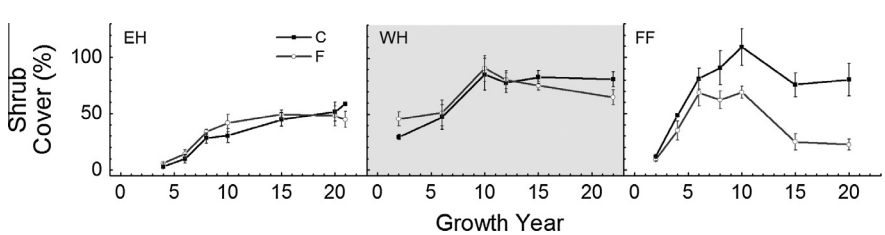


**Fig. 3.** Shrub coverage of C and F treatments at three sites. Error bars show SE.

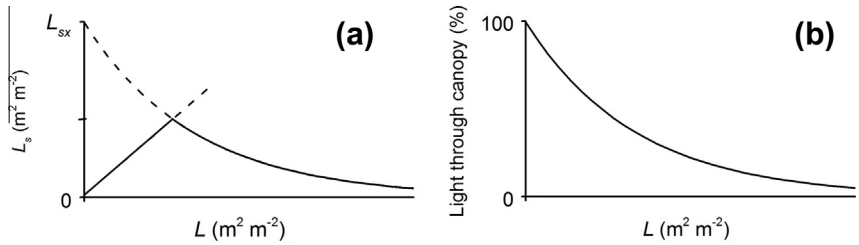


**Fig. 4.** A new function (Eqs. (16) and (17)) was added to 3-PG for estimating shrub LAI ($L_S$) from tree LAI ($L$) (a). We assumed a fixed ratio ($K_L$) of $L_S/L$ at stand establishment (Eq. (16)). After light became a limiting factor for shrub growth, we assumed that the rate of change in $L_S$ (a) is proportional to the change of light penetrating tree canopy (b); $L_S$ was then estimated by applying Beer's law (Eq. (17)) (a).

lowed for calibration of the functions to fit the actual shrub growth. Parameter $K_L$ describes how fast the shrub LAI will reach its maximum point, after which shrub LAI is limited by light; imagine increasing the slope of the straight line in Fig. 4a as $K_L$ increases. $L_{SX}$ delineates how the $L_S$ changes with $L$ when light is limiting under the tree canopy; imagine moving $L_{SX}$ higher and drawing another curve higher than the old one as $L_{SX}$ increases in Fig. 4a. Both $K_L$ and $L_{SX}$ determine peak $L_S$. Moreover, simply setting $K_L = 0$ turns off the shrub function. We only had one-time measurements of shrub LAI (Fig. 5p–r), so we first assumed $K_L = 1$ and tuned $L_{SX}$; we then considered tuning $K_L$ only if necessary. By tuning, we mean an *a posteriori* adjustment of a parameter to improve fit without reference to empirical estimates of the parameter value. We tried to minimize such tuning throughout this study.

### 2.7. Climate data

Climate data were available at all three sites. Short-term meteorology stations were installed at EH (June 2005 to August 2007) and FF (April 2005 to October 2007). A long-term meteorology station (NESS ID: CA20C0AA) has collected data since 1990 at WH. Available data at the three sites include air temperature, precipitation, relative humidity (RH), and solar radiation. We extrapolated the whole climate dataset to the year of plantation establishment (see Appendix A). We used multiple regressions with surrounding stations to extend air temperature and precipitation, except that precipitation data of site EH were substituted by a nearby site (see Appendix A). Missing solar radiation data were modeled using a temperature-based model (Bristow and Campbell, 1984) that was well calibrated by existing data (see Appendix A). PAR data were available at site EH and FF. PAR equaled 56% of the energy in solar radiation at both sites ($P < 0.001$, $R^2 > 0.99$). VPD was estimated from observed temperature and RH, or from daily minimum and maximum temperature if RH was not available (see Appendix A).

### 2.8. Field and lab measurements

Multiple inventories provided growth data at plantation ages 2, 4, 6, 8, 10, 15, and 20 years. Tree height, diameter, crown length, and crown width were measured for 20 trees in each measurement plot. When trees were smaller than 1.4 m height, diameter at 10 cm from ground was measured. Volume was estimated with DBH and tree height if tree height was >1.4 m (Oliver and Powers, 1978). Otherwise, volume was calculated regarding the tree as a cone. Aboveground biomass was estimated with allometric equations. These were either from Zhang et al. (2010) for trees taller than BH (1.4 m) or from Powers et al. (2013) for trees shorter than BH. LAI was calculated with total leaf biomass estimated from specific leaf area (SLA) (Xu et al., 2001) and an allometric equation developed for the GOE study (unpublished data). Sapflow was measured in the HF treatment in 2007, using six trees per stand (unpublished data).

Quantum yields were measured for all treatments at our sites following Nippert and Marshall (2003). Briefly, one-year-old sun and shade foliage was collected by tree-climbing from three trees per treatment per site, one block each. A LiCor LI-6400 portable photosynthesis system was used to measure net $CO_2$ assimilation (A) of foliage at eight decreasing levels of photosynthetically active radiation (PAR): 1500, 750, 250, 75, 50, 30, 10 and 0 μmol m$^{-2}$ s$^{-1}$). Data were fitted using non-linear regression to a non-rectangular hyperbola (Hanson et al., 1987). The slope of the resulting regression at $A = 0$ was used to estimate quantum yield. The slope at $A = 0$ was used because the quantum yield was near maximum and the value was better constrained than at a point with unknown internal $CO_2$ concentration (Nippert and Marshall, 2003).

Tree ring $\delta^{13}C$ was measured for each treatment and site. Twelve trees were sampled for tree rings at each site, one per block. Tree ring widths were measured and crossdated among trees using program COFECHA to guarantee the dating of rings (Holmes, 1983). Values of $\delta^{13}C$ were measured for individual rings from 1995 (1994 at FF) to 2004 at Idaho Stable Isotopes Lab, University of Idaho with a NC 2500 EA (Carlo Erba Instruments, Milan, Italy) coupled to a mass spectrometer (Delta$^+$ IRMS, Finigan MAT, Bremen, Germany). Results were expressed in delta notation relative to the Vienna Pee Dee Belemnite (VPDB) standard. Wood samples were pretreated to remove mobile extractives such as resins, oils, and some inorganic salts and hemicelluloses; the holocellulose and lignin remained in the sample (Harlow et al., 2006). This method was comparable to traditional wood extraction methods, which retain only holocellulose (HC) (Harlow et al., 2006). In a preliminary test of this method, we further tested both methods using ponderosa pine samples from one tree at WH site. The $\delta^{13}C$ values were correlated ($R^2 = 0.99$, $P < 0.001$) using the two methods; the $\delta^{13}C$ using the traditional HC method was 1.10‰ higher than that using the extractive-free method (paired-*t* test, $P < 0.001$). This confirmed the earlier results of Harlow et al. (2006).

We collected phloem contents and measured their $\delta^{13}C$ at WH site. Tree cores (1 cm in length) were extracted from three trees per treatment in July 2011. Tree cores were separately placed in 15 mM pH = 7 phosphate-glass solution and phloem contents were allowed to exude for 8 h (Gessler et al., 2004). The solution was dried in the oven at 70 °C and the solid material was tested for $\delta^{13}C$.

### 2.9. Model parameterization and calibration

We used field measurements as model parameters whenever they were available. These parameters included quantum yields, SLA, and parameters for allometric equations. Initial biomass for foliage, root, and stem was set to 1.5, 1.4, and 0.9 kg ha$^{-1}$ respectively, which was estimated from the planted seedlings (Zhang et al., 1996). As some mortality occurred after planting (Powers et al., 1992), the initial stocking was set as the number of surviving trees at ~14 years of stand age. One of four soil types in 3-PG was

assigned to each site based on the sand and clay content (Table 1) (EH, sandy loam; WH, clay loam; FF, clay).

We used both observed soil moisture and transpiration as references to parameterize the maximum available soil water ($ASW_{max}$). Observed soil moisture (10 cm and 40 cm depths, unpublished data) decreased sharply in May and stabilized at a low level in June–September at all three sites (data not shown); the low soil moisture limited the transpiration at site EH and WH in June–September, but the trees at FF still transpired a significant amount of water despite the dry soil during this period (Fig. 6c). This suggested that the FF trees extract water from deeper soils than the depth of the soil moisture sensors during this time. We hence calibrated the $ASW_{max}$ at each site such that the simulations would match the observed depletion of soil moisture and declining transpiration.

Besides soil moisture and transpiration, we used six observed items to calibrate or tune the model. These included: phloem $\delta^{13}C$, tree ring $\delta^{13}C$, DBH, tree LAI, shrub LAI, and stand volume. We defined calibration as an *a priori* modification of the model parameters to fit observations (phloem $\delta^{13}C$ and tree ring $\delta^{13}C$); tuning was *a posteriori* (DBH, tree LAI, shrub LAI, and stand volume). The $\delta^{13}C$ submodel provided a new approach to parameterize 3-PG (Wei et al., 2014). When inappropriate parameters were used for simulations of carbon assimilation and canopy conductance, incorrect $\delta^{13}C$ simulations could reveal the errors. These model parameters included $\alpha_{cx}$ and $g_{cmax0}$. Observed DBH was used as the reference to tune a gas-exchange parameter, $k_{g0}$. Two background parameters ($p_{B0}$, and $p_{B1}$, see Table 3) were tuned to fit volume simulations to observations. Tree LAI was used as the reference to tune an allocation parameter, $p_{20}$. Shrub LAI was used to tune $L_{sx}$ and $K_L$. We also used some default values and gleaned some parameters from earlier 3-PG simulations for ponderosa pine (see Table 2).

The $\delta^{13}C$ submodel constrained our parameterization of the model. The gas-exchange parameter $g_{cmax0}$ was first calibrated at site WH to fit $\delta^{13}C$ of new photosynthate to phloem $\delta^{13}C$. The

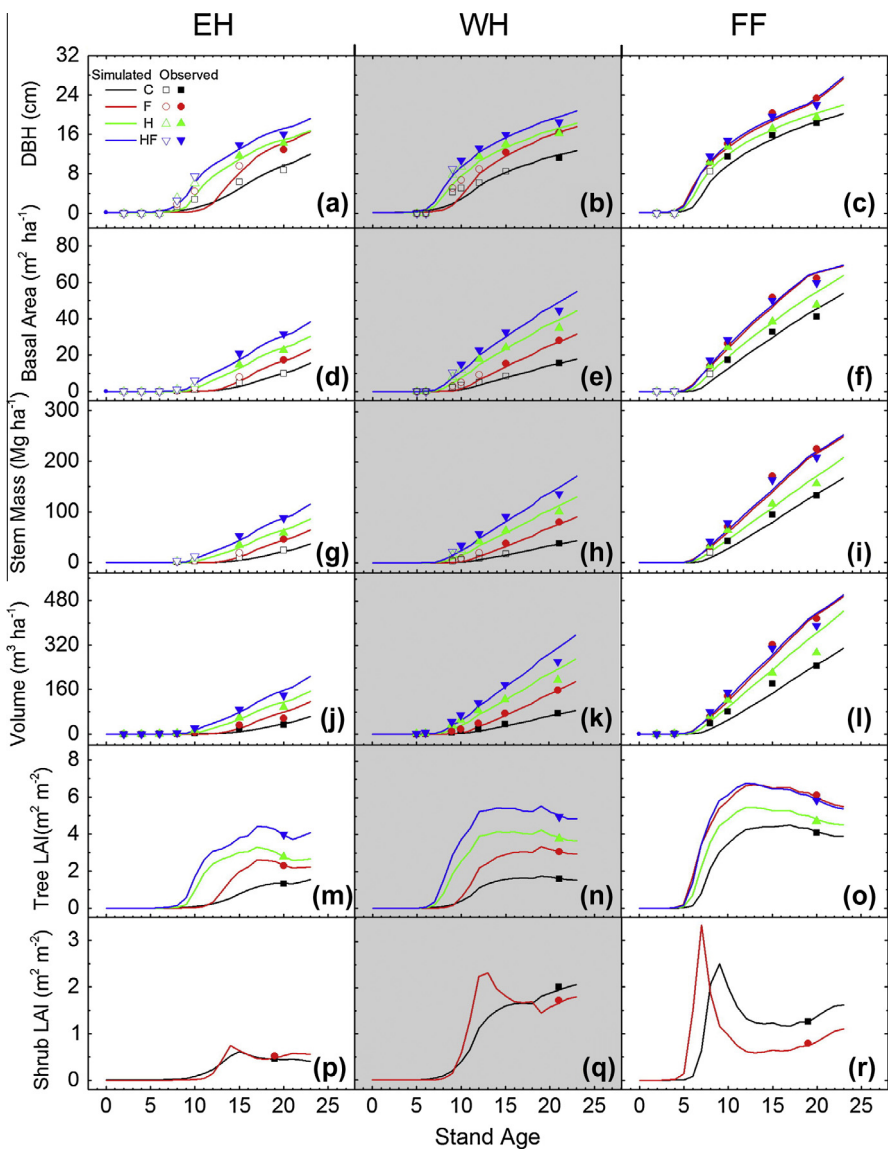


**Fig. 5.** Simulations and observations of DBH, basal area, stem mass, volume, tree LAI, and shrub LAI for three study sites (EH, WH, and FF). Four treatments were modeled at each site. Lines are model simulations and points are observed field data. When trees were small and could not be measured at breast height, tree diameter was measured either at 5 cm above ground for all trees or at diameter height for only big trees. Almost all trees passed breast height when stand average DBH ≈ 10 cm, so we marked DBH and DBH-based estimations with open symbols when trees were small. We calibrated the model to fit simulations to observed DBH, Volume, and LAI. The model simulations overestimated the growth near the end of the simulation at more productive plots.

simulation of $\delta^{13}C$ was sensitive to $\alpha_{cx}$ and $g_{cmax}$ (Wei et al., 2014). As $\alpha_{cx}$ was measured onsite, only $g_{cmax0}$ required calibrating. When simulated $\delta^{13}C$ of new photosynthate fitted phloem $\delta^{13}C$, we estimated the mean annual tree ring $\delta^{13}C$ when $\varepsilon_{sp} = 0$. The difference between this value and mean measured tree ring $\delta^{13}C$ was used as $\varepsilon_{sp}$. Because $\delta^{13}C$ simulations may not be reliable when LAI < $L_x$ (Wei et al., 2014), we only used data in years with LAI $\geqslant L_x$ for calibration. The phloem $\delta^{13}C$ was not measured at site EH and FF, and hence we calibrated these two sites differently. We assumed that $\varepsilon_{sp}$ was constant across sites, and hence used the $\varepsilon_{sp}$ estimation from site WH. Tree ring $\delta^{13}C$ was used to calibrate $g_{cmax0}$ for sites EH and FF.

Least-squares approaches were used to tune the model. The sum of squared residuals (SSR) between model outputs and measurements, $\sum(\text{Simulation} - \text{Measurement})^2$, was used to find the best parameter value, which was obtained when SSR reached minimum. Parameters were tuned stepwise with predetermined increments or decrements: $g_{cmax0}$, 0.001 m s$^{-1}$; $k_{g0}$, 0.001 mBar$^{-1}$; $p_{20}$, $p_{B0}$, and $p_{B1}$ 0.01; $L_{SX}$, 0.1 m$^2$ m$^{-2}$; $K_L$, 0.1; $ASW_{max}$, 10 mm; and fertility rating, 0.1 (see Table 3 for abbreviations).

### 2.10. Sensitivity test

We ran a simple sensitivity test to estimate the impact of possible errors in $\delta^{13}C$ calculation on biomass simulations. We tested the responses of tree ring $\delta^{13}C$ and aboveground biomass to the change of $g_{cmax0}$ at HF treatments of site WH and FF. We changed the $g_{cmax0}$ value to create scenarios that led to $\delta^{13}C$ being inappropriately estimated. In these simulations, parameter $g_{cmax0}$ was changed by ±0.001 and ±0.002 m s$^{-1}$ from the initial value.

### 2.11. Statistical analysis

We tested the effect of different treatments on quantum yields using analysis of variance (ANOVA). We treated each site as a split plot, and the statistical model was:

$$y_{ijklm} = \mu + \alpha_i + \eta_{j(i)} + \beta_k + \alpha_i\beta_k + \gamma_{l(ik)} + \varepsilon_{ijklm} \quad (19)$$

where $y_{ijklm}$ represents an individual experimental unit response, $\mu$ is the population mean, $\alpha_i$ is the effect of $i$th sites, $\eta_{j(i)}$ is the whole plot level random error, $\beta_k$ is the effect of $k$th treatments, $\alpha_i\beta_k$ is the interaction of sites and treatments, $\gamma_{l(ik)}$ is the effect of canopy positions, and $\varepsilon_{ijklm}$ is the split-plot level random error. $\eta_{j(i)}$ is nested in $\alpha_i$, and $\gamma$ is nested under $\alpha_i\beta_k$. The statistical program SAS was used for the test. Proc MIXED was used for ANOVA. Proc REG was used in the linear regressions used to extrapolate the climate data.

## 3. Results

### 3.1. Quantum yields

Quantum yields were consistent across the three sites. The ANOVA results showed that there was no significant difference between canopy positions or among treatments at the 0.1 level. Interactions were also not significant at the 0.1 level. This indicated that fertilizer did not change the quantum yield. So we turned off the effect of fertility rating on photosynthesis, allowing the fertility rating only to change carbon allocation. However, the quantum yields were different among sites at the 0.1 level ($P = 0.08$). We hence used different quantum yields across sites. The average quantum yields were 0.056 (0.003 SE), 0.049 (0.003), and 0.048 (0.004) μmol $CO_2$ mol$^{-1}$ incident PAR at sites EH, WH, and FF, respectively.

### 3.2. Canopy closure

The new canopy closure function reasonably fitted the observed data of all treatments, except the C and F treatments at sites EH and WH (Fig. 2). The fitted exponent was 2.6 and the fitted $t_{cc}$ values are shown in Table 3. The observed canopy cover after the 10th year slightly diverged from the trajectory that was determined using observations before the 10th year at the F treatment at site EH and WH (Fig. 2). We still used the 2.6-power curve for these two F treatments as the discrepancies were minor.

### 3.3. $\delta^{13}C$ measurements and simulations

The measured phloem $\delta^{13}C$ values at WH were −27.3‰ (0.3 SE), −27.4‰ (0.2), −27.1‰ (0.2), and −26.5‰ (0.1) for treatment C, F, H, and HF respectively for July 2012. The value at the HF treatment was significantly higher than in the other treatments at the 0.05 level.

We calibrated $g_{cmax0}$ to fit the simulated $\delta^{13}C$ of new photosynthate to measured phloem $\delta^{13}C$. Using $\delta^{13}C$ data when tree LAI $\geqslant L_x$, the mean $\varepsilon_{sp}$ (Eq. (13)), which describes the difference between tree rings and phloem contents, was determined to be 1.7‰ based on simulations at the H and HF treatments.

Observed and simulated $\delta^{13}C$ are shown in Fig. 7. Observed tree ring $\delta^{13}C$ variations were small among our study sites: EH, −25.3 (0.1 SE); WH, −25.3 (0.06); and FF −26.5 (0.1) ($N = 119$, 120, and 132 individual tree ring respectively). For all years when LAI $\geqslant L_x$, the mean absolute difference ranged from 0.23‰ to 0.83‰ between simulations and measurements across all treatments at sites WH and FF. Because LAI did not exceed $L_x$ in the C, F, and H treatments at site EH and $\delta^{13}C$ submodel did not function well under these conditions, we did not show $\delta^{13}C$ data for EH.

### 3.4. Model parameterization and calibration

Parameters that were identical across all simulations are shown in Table 2. Table 3 shows site- and treatment-specific parameters.

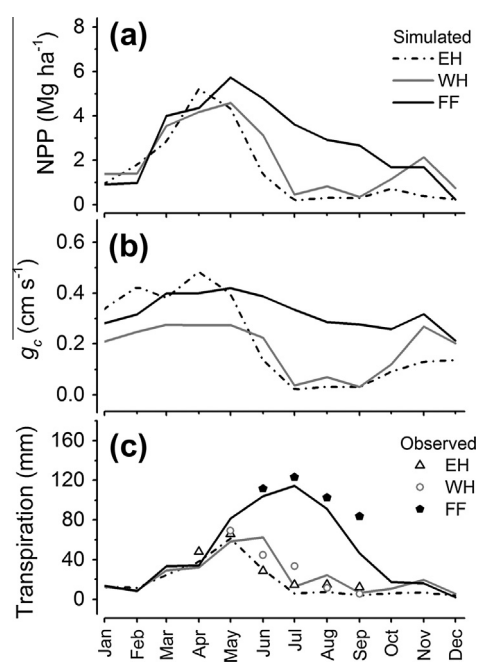


**Fig. 6.** Site differences in monthly NPP, canopy conductance ($g_c$), and transpiration in 2007. Only data from HF treatments were shown. Lines are model simulations and dots are sapflux-based transpiration. Trees at FF kept transpiring larger amount of water than at other two sites, and hence had higher monthly NPP in most months.

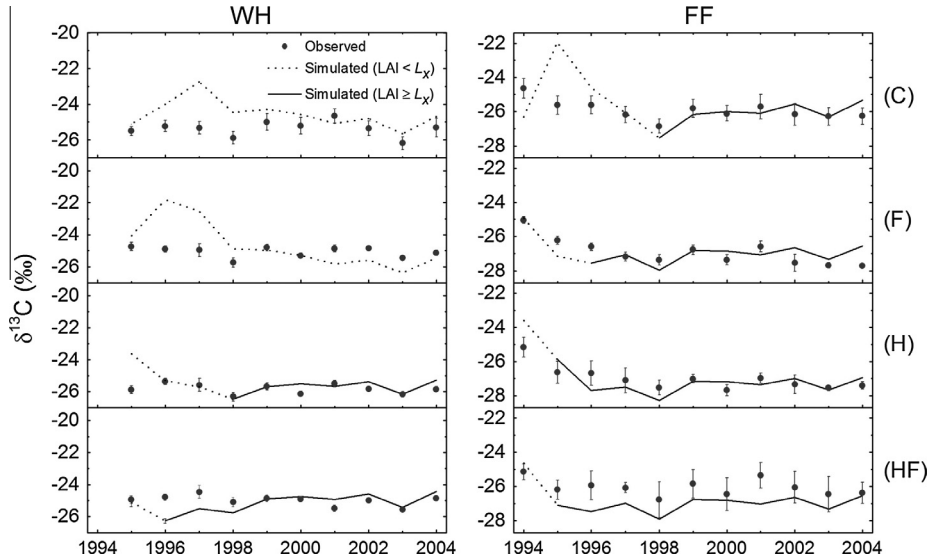


**Fig. 7.** Simulated and observed annual tree ring $\delta^{13}$C. $\delta^{13}$C values were marked differently for the period that tree LAI < $L_x$ or tree LAI ⩾ $L_x$. Error bars show SE.

Parameters differed among sites and treatments for shrub growth ($L_{SX}$ and $K_L$), canopy conductance ($k_{g0}$ and $g_{cmax0}$), and carbon allocation to foliage ($p_2$ and $p_{20}$). $L_{SX}$ was related to site index, with higher $L_{SX}$ values at the more productive sites or treatments. Herbicide treatments (H and HF) were generally more productive and less sensitive to VPD change (i.e., lower $k_g$ value) than non-herbicide treatments. This indicated that trees maintained higher canopy conductance, transpired more water, and hence maintained higher productivity at herbicide-treated plots than controls. Only the F treatment at site FF was an exception. This site had a lower $k_{g0}$ value and higher productivity than all other treatments at site FF, including HF.

### 3.5. Simulations vs. observations

After calibration, the model reasonably simulated the forest growth of each treatment in terms of DBH, stem mass, basal area, and volume (Fig. 5). We also fit leaf and shrub LAI simulations to the single observation at each treatment. The variations of simulated shrub LAI were similar to observed shrub coverage (Fig. 3). Simulated shrub LAI and observed shrub coverage peaked at similar times for the F treatments. The biomass accumulation was near zero before $t_{cc}$ (Fig. 5). The new canopy closure function allowed less light for trees than the original linear function at any given $t_{cc}$ value. The low-growth periods matched the observations and validated the canopy closure function. It was possible to use 3-PG to simulate the growth of fertilizer and herbicide treatments with the new shrub and canopy closure functions and still keep the model simple.

We compared the simulations with and without changing $g_{cmax}$ and $k_g$ with tree height (Fig. 8). We picked the highly productive HF treatment at site FF to demonstrate the difference, and we used identical parameters for both simulations with and without the change. The simulations without the change had much higher simulation for DBH than with the change, especially toward the end of the simulations.

Simulated transpiration was 19%, 0%, and 20% lower than sapflux observations at the HF treatments of site EH, WH, and FF respectively (Fig. 6c). Recall that the simulations of transpiration were calibrated against $\delta^{13}$C, but not against sap flux. If we calibrated transpiration against sap flux, the value for $g_{cmax0}$ would be only 0.001, 0, 0.002 m s$^{-1}$ higher at site EH, WH, FF respectively. Therefore, this agreement serves as a successful test of calibration using the $\delta^{13}$C submodel in situations where sapflux data are not available.

### 3.6. Site differences

The three sites differed in NPP, canopy conductance, and transpiration. We presented simulations of HF treatments to avoid the confounding of differences in soil fertility and understory conditions among sites; we took 2007 (stand age 20 at site EH and FF, and 22 at site WH) as an example because transpiration was measured this year (Fig. 6). The simulated annual NPP was 18.7, 23.9, and 33.6 Mg ha$^{-1}$, and annual transpiration was 212, 282, and 518 mm at site EH, WH, and FF, respectively. The most productive site FF transpired far more water and kept higher canopy conductance and NPP throughout the summer of 2007 (May–September). In contrast, NPP, transpiration, and canopy conductance all approached zero in mid-summer at the two less productive sites, EH and WH (Fig. 6). Although these NPP values seem high, it is important to note that these stands were accumulating as much as 200 Mg ha$^{-1}$ of stem mass within twenty years (Fig. 5i); this is far more than is typical for unmanaged ponderosa pine stands.

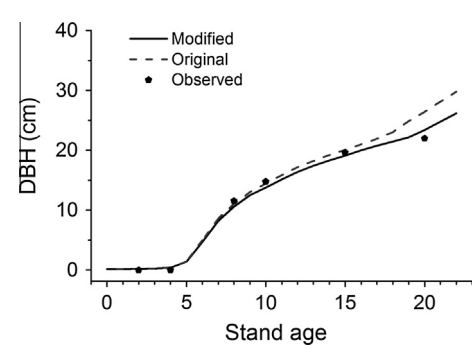


**Fig. 8.** Comparison of the DBH simulations with (modified) and without (original) $g_{cmax}$ and $k_g$ changing with tree height. All other parameters were identical between two simulations. Dots show the observed DBH.

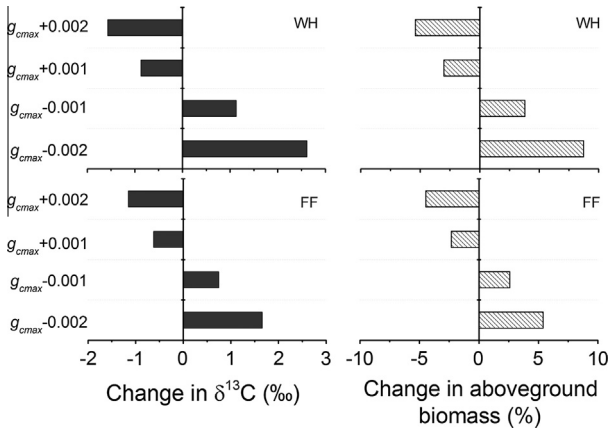


**Fig. 9.** Results of the sensitivity test. We tested the responses of tree ring $\delta^{13}C$ and aboveground biomass to $g_{cmax0}$. $g_{cmax0}$ was changed by ±0.001 m s$^{-1}$ and ±0.002 m s$^{-1}$ from the finalized values of HF treatments at site WH and FF, respectively. Presented data were the changes from the simulations using original parameter values. The changes of both parameters were significantly correlated $R^2 > 0.99$ and $P < 0.01$ at both sites; WH: $y = 0.032x$; FF: $y = -0.002 + 0.035x$; $x$ is the change of $\delta^{13}C$ (‰) and $y$ is the percent change in aboveground biomass. Therefore, in the tested range, 1‰ error in the tree ring $\delta^{13}C$ was related to 3.2% and 3.5% of error in aboveground biomass at site WH and FF respectively. We believe it is very easy to detect a 1‰ error in the tree ring $\delta^{13}C$, but not easy to detect a 4% error in aboveground biomass.

### 3.7. Sensitivity test

The sensitivity test estimated the connection between wrongly estimated $\delta^{13}C$ and wrongly estimated aboveground biomass (Fig. 9). Increasing $g_{cmax0}$ reduced $\delta^{13}C$ and aboveground biomass, and decreasing $g_{cmax0}$ increased $\delta^{13}C$ and aboveground biomass at site WH and FF. The relationship between the change in $\delta^{13}C$ and change in aboveground biomass was linear in the tested range ($R^2 > 0.99$ and $P < 0.01$ at both sites); higher change in $\delta^{13}C$ was related to higher change in aboveground biomass (Fig. 9). If there was ~1‰ error in $\delta^{13}C$ estimation, the model would cause almost 4% error in the estimation of aboveground biomass at site WH and FF. This indicated that the $\delta^{13}C$ submodel was usefully constraining the model parameterization.

## 4. Discussion

We employed a parsimonious approach to represent site and treatment differences in the model. In this study, 3-PG simulated forest growth in a wide range of climate, fertility, water availability, and competing vegetation composition. There were 13 parameters that differed across the treatments or among sites (Table 3); these were especially parameters controlling allocation and gas exchange (Table 3). The gas-exchange parameters were tested with the $\delta^{13}C$ submodel (Fig. 7), which assured their reliability. Moreover, we introduced two additional means to describe the treatment effects in the model: estimating understory water consumption and assigning different canopy closure time.

The new empirical canopy closure function well represented the process for most treatments at the three sites. The canopy closed earlier at more productive sites and treatments (Fig. 2, Table 3). Canopy closure closely followed a trajectory with a 2.6-power curve as it approached maximum shrub cover, except for the C and F treatments at site EH and WH. Apparently, the dry sites without vegetation control diverged from this curve (Fig. 2), which may be related to low canopy growth rate of trees when they competed with the shrubs (Shainsky and Radosevich, 1986). A possible solution is constructing mechanistic connections between foliage production and canopy closure. The low foliage production could then restrict the canopy closure if the environment was harsh or shrub competition was severe.

Our preliminary shrub functions reasonably estimated shrub growth, despite the simple model structure. The functions were also flexible enough to allow finer tuning if detailed field shrub measurements were available. There are some limits of the simple light-driven functions. First, shrub growth may also be limited by belowground factors in ponderosa pine forests, e.g., water and nutrients (e.g. Riegel et al., 1992). Second, sunflecks complicate the understory light environment, and a forest canopy with complex structure may support more understory growth than a single-layer canopy with the same LAI (Van Pelt and Franklin, 2000; Battaglia et al., 2002). In our case, the canopy structure was relatively simple given that these were even-aged, monoculture plantations; these are the conditions for which 3-PG was developed (Landsberg and Waring, 1997).

Both measurements and simulations of forest growth reflected the benefit of competing vegetation control and fertilizer, and the productivity within a site generally followed the order C < F < H < HF. The only exception was F vs. HF at site FF. Even without herbicide, the F treatment had higher productivity than the HF treatment at site FF. Two facts may possibly explain this: (1) the competition of the understory for soil moisture was minor at FF site, as soil moisture was abundant and fast development of a forest canopy limited the growth of shrubs; (2) in the absence of herbicide, N-fixing *Ceanothus* on the F treatment increased whole soil N by 8% in 16 years (McFarlane et al., 2010), which may have increased N availability to the tree canopy as well; and (3) decomposition of shrubs may provide additional nutrients, and the soil quality would be higher in non-vegetation controlled plots than vegetation controlled plots in terms of soil carbon, nitrogen, and microbial biomass (Busse et al., 1996).

We replaced the original age modifier in 3-PG with tree-height based functions. Although the productivity varied dramatically among treatments and sites, one set of parameters for the height-functions worked for all treatments and sites (Figs. 5 and 8). In contrast, if we had used the original age modifier, we would have had to set different parameters for each treatment and site. Apparently, both $g_{cmax}$ and $k_g$ changed with tree height based on three studies for ponderosa pine (Hubbard et al., 1999; Ryan et al., 2000; Law et al., 2001). However, these three studies each measured only two height classes. We assumed linear changes of $g_{cmax}$ and $k_g$ with tree height, which worked reasonably in our study (Fig. 8), where the tree height was fairly low and the maximum mean stand tree height was only 14.6 m at FF sites at stand age 20. However, descriptions of changing $g_{cmax}$ and $k_g$ with height remain limited; these linear patterns should only be used with caution.

A physiological growth model that is correctly parameterized can provide insights into the reasons for growth differences. The pronounced differences at the GOE sites provide a unique opportunity. We found that the Feather Falls sites were subsidized by a deep water source, which maintained high transpiration rates throughout the summer drought, giving trees much higher GPP than on the other two sites. This initially favored growth of shrubs as well as trees, but the trees grew so rapidly above the shrubs that they began to shade them out relatively soon. The herbicide treatments shifted allocation toward foliage; the latter resulted in a compounding of growth as the canopy developed. The fertilization increased growth by an increase in foliage allocation. The combination of fertilizer and herbicide was assigned the highest foliage allocation and, when combined with the rechanneling of water and light to the trees, gave rise to the highest productivity among the treatments. Although these site and treatment differences are partially the result of model tuning, the tuning was done with a realistic model parameterized with as much real site data as

possible and constrained by the isotopic data. In short, it seems reasonable to think that these inferences about the causes of different growth rates are rigorous and sound.

The $\delta^{13}C$ submodel (Wei et al., 2014) tested the reliability of gas exchange parameters, including $\alpha_{cx}$ and $g_{cmax}$ ($g_{cmax0}$ in this study). Many 3-PG studies (e.g. Sands and Landsberg, 2002; Swenson et al., 2005; Paul et al., 2007; Xenakis et al., 2008) have used the default parameters in Landsberg and Waring (1997) for $g_{cmax}$ (i.e. 0.02 m $s^{-1}$); some studies have calibrated $g_{cmax}$ based on changes in soil moisture (Landsberg et al., 2003), or have estimated them from observed stomatal/canopy conductance (Whitehead et al., 2002; Almeida et al., 2004). As to $\alpha_{cx}$, previous studies have generally either calibrated this parameter with biomass production or used the default value (e.g. Sands and Landsberg, 2002; Whitehead et al., 2002; Landsberg et al., 2003; Almeida et al., 2004; Swenson et al., 2005; Paul et al., 2007; Xenakis et al., 2008). We applied a recently introduced approach that measured $\alpha_{cx}$, and calibrated $g_{cmax}$ using the $\delta^{13}C$ submodel by comparing simulated $\delta^{13}C$ to tree ring $\delta^{13}C$. This approach can provide a convenient test for the model parameterization (Fig. 7), because $\delta^{13}C$ in tree rings are easily obtained.

There are some limits to this version of the $\delta^{13}C$ submodel. First, possible errors may occur from using the simple model (Eq. (10)) to estimate $\delta^{13}C$. Some factors were ignored in the simplified model, including fractionations related to respiration, photorespiration, and mesophyll resistance (Farquhar et al., 1982). A study estimated that the possible error was 0.4‰ when using the simplified model compared with a complete model that included those factors based on three coniferous species in northern Idaho (Ubierna and Marshall, 2011). Secondly, the $\delta^{13}C$ submodel did not function well before canopy closure and when LAI < $L_x$ (Fig. 7). This deficiency of the $\delta^{13}C$ submodel lies in the structure of 3-PG, which treats the canopy as a "big leaf" (Farquhar, 1989). When $t < t_{cc}$, the big leaf has not yet formed; when LAI < $L_x$, the big leaf is breaking up (Eq. (6)). Third, $\varepsilon_{sp}$ may change across months and years. In a study that addressed this issue for evergreen species (Gessler et al., 2009), $\varepsilon_{sp}$ was nearly constant, but not statistically so (Arthur Gessler, personal communication). As discussed in Wei et al. (2014), further physiological studies are necessary to solve these problems.

## 5. Conclusions

We parameterized and modified a simple process-based forest model to simulate the growth of ponderosa pine at three plantation sites. We introduced new functions to consider the changes of gas exchange with tree height. We also created new functions to estimate shrub competition in the presence and absence of herbicide treatments. A $\delta^{13}C$ submodel was used to assist parameterization and test the physiology embedded in the model. This modeling project not only fulfilled a long-standing objective of the longer-term GOE project, but also developed an innovative means to use a physiological trait of trees (i.e. $\delta^{13}C$) to constrain model parameterization and therefore simulations of forest production. Although $\delta^{13}C$ is not a common term used in forest management, it could be a powerful tool in the foresters' toolbox, aiding in the realistic parameterization of process-based models in the future.

## Acknowledgments

We thank Therese Alves, Bob Carlson, Gary Fiddler, Donald Jones, Carol Shestak, Bert Spear, David Young (all in Pacific Southwest Research Station – Redding), and others who helped install, maintain, and measure these GOE plots during the last 20 years. We also thank Allen Tedrow, and lab managers of Idaho Stable Isotopes Lab, Margaret Ward and Benjamin Miller, for processing tree ring $\delta^{13}C$ samples. Special thanks to Richard Waring, Joe Landsberg, and Peter Sands for their insightful and supportive comments to this study. The Sierra Cascade Intensive Forest Management Research Cooperative and Sierra Pacific Industries provided partial financial support for the project.

## Appendix A. Climate data

Monthly precipitation and temperature data were extended based on multiple regressions between modeling sites and surrounding meteorological stations. We searched data from National Climatic Data Center (www.ncdc.noaa.gov) and picked meteorology stations within 60 km of the modeling sites with records dated back to 1986. We kept stations with fewest missing data and picked four meteorological stations for each modeling sites. Multiple regressions were constructed using Akaike Information Criterion between observed precipitation, $T_{min}$, $T_{max}$, and $T_{ave}$ at modeling sites and their counterparts at reference meteorological stations. When a missing data presented at one station, the best model without using that station was used as replacement. All models but one had $P$ value <0.001, with adjust $R^2$ value at least 0.97, 0.89 and 0.95 for temperatures at WH, EH, and FF respectively, and 0.92 and 0.96 for precipitation at WH and FF respectively. However, the precipitation model for EH was not significant at the 0.05 level, mainly due to the fact that there were only 19 month of broken observed data. We used the precipitation at a station (Orland, CA, USC00046506, 77 ma.s.l.) as the surrogate; this station was the closest station to site EH and located in the same rain shadow area as site EH.

Solar radiation ($Q$) was measured for some years at three sites, and was modeled for the rest of the years. A temperature based radiation model (Bristow and Campbell, 1984) was used to estimate daily transmissivity ($T_t$) and solar radiation ($Q$):

$$Q = Q_0 T_t = Q_0 A_t (1 - \exp(-B_t \Delta T^{C_t}) \quad (A.1)$$

where $Q_0$ is the extraterrestrial solar radiation, $A_t$ is the maximum daily clear sky transmissivity, $\Delta T$ is the range in daily temperature (*i.e.*, $T_{max}$–$T_{min}$ with rain adjustments, see Bristow and Campbell, 1984 for detail), and $B_t$ and $C_t$ are empirical coefficients describing how soon maximum $A_t$ is achieved as $\Delta T$ increased. To estimate $\Delta T$, we extended daily $T_{min}$ and $T_{max}$ using the same approach as extending monthly temperature (all $P < 0.001$, adjust $R^2$ for $T_{min}$ and $T_{max}$ respectively: 0.41 and 0.59 at EH, 0.91 and 0.97 at FF, and 0.86 and 0.96 at WH). A $A_t$ value of 0.80 was used across three sites, which is the maximum daily transmissivity observed. We used the default value (2.4) for $C_t$. The last parameter, $B_t$, determines the seasonal responses of $T_t$ to $\Delta T$ as:

$$B_t = m_{t1} \exp(m_{t2} \overline{\Delta T}) \quad (A.2)$$

where $\overline{\Delta T}$ is the monthly mean $\Delta T$, and $m_{t1}$ and $m_{t2}$ are constants. We calibrated $m_{t1}$ and $m_{t2}$ at each site to fit the simulations to observed $Q$ using the least square approach. In the calibration periods (1999–2012 at WH, 2005–2007 at EH and FF), the simulated monthly $Q$ explained 94%, 99%, and 98% of the variation of the observations at EH, FF, and WH respectively.

Daily daylight vapor pressure deficit (VPD, kPa) was averaged from observations from sunrise to sunset. In order to extend the VPD dataset for unmeasured periods, we calculated a surrogate VPD ($V_T$) based on monthly $T_{min}$ and $T_{max}$ as:

$$V_T = e_{s(T_{max})} - e_{s(T_{min})} \quad (A.3)$$

This calculation assumed that $T_{min}$ reaching dew point, which did not always stand. We then corrected $V_T$ by using linear regression between measured daytime VPD ($V$) and $V_T$. The linear

equations (all $P < 0.001$) are $V = 0.062 + 0.831V_T$ at EH ($N = 26$, $R^2 = 0.78$), $V = -0.042 + 0.781V_T$ at FF ($N = 31$, $R^2 = 0.99$), and $V = -0.012 + 0.90V_T$ at WH ($N = 265$, $R^2 = 0.96$).

## References


Almeida, A.C., Landsberg, J.J., Sands, P.J., 2004. Parameterisation of 3-PG model for fast-growing Eucalyptus grandis plantations. Forest Ecology and Management 193, 179–195.

Battaglia, M., Sands, P.J., 1998. Process-based forest productivity models and their application in forest management. Forest Ecology and Management 102, 13–32.

Battaglia, M.A., Mou, P., Palik, B., Mitchell, R.J., 2002. The effect of spatially variable overstory on the understory light environment of an open-canopied longleaf pine forest. Canadian Journal of Forest Research 32, 1984–1991.

Bristow, K.L., Campbell, G.S., 1984. On the relationship between incoming solar radiation and daily maximum and minimum temperature. Agricultural and Forest Meteorology 31, 159–166.

Busse, M.D., Cochran, P.H., Barrett, J.W., 1996. Changes in ponderosa pine site productivity following removal of understory vegetation. Soil Science Society of America Journal 60, 1614–1621.

Campbell, G.S., Norman, J.M., 1998. Introduction to Environmental Biophysics. Springer, New York.

Coops, N.C., Waring, R.H., 2001. Assessing forest growth across southwestern Oregon under a range of current and future global change scenarios using a process model, 3-PG. Global Change Biology 7, 15–29.

Coops, N.C., Waring, R.H., Law, B.E., 2005. Assessing the past and future distribution and productivity of ponderosa pine in the Pacific Northwest using a process model, 3-PG. Ecological Modelling 183, 107–124.

Farquhar, G.D., 1989. Models of integrated photosynthesis of cells and leaves. Philosophical Transactions of the Royal Society of London. B, Biological Sciences 323, 357–367.

Farquhar, G.D., Sharkey, T.D., 1982. Stomatal conductance and photosynthesis. Annual Review of Plant Physiology 33, 317–345.

Farquhar, G., O'Leary, M., Berry, J., 1982. On the relationship between carbon isotope discrimination and the intercellular carbon dioxide concentration in leaves. Functional Plant Biology 9, 121–137.

Fisher, J.B., Baldocchi, D.D., Misson, L., Dawson, T.E., Goldstein, A.H., 2007. What the towers don't see at night: nocturnal sap flow in trees and shrubs at two AmeriFlux sites in California. Tree Physiology 27, 597–610.

Gessler, A., Rennenberg, H., Keitel, C., 2004. Stable isotope composition of organic compounds transported in the phloem of European beech – evaluation of different methods of phloem sap collection and assessment of gradients in carbon isotope composition during leaf-to-stem transport. Plant Biology 6, 721–729.

Gessler, A., Brandes, E., Buchmann, N., Helle, G., Rennenberg, H., Barnard, R.L., 2009. Tracing carbon and oxygen isotope signals from newly assimilated sugars in the leaves to the tree-ring archive. Plant, Cell & Environment 32, 780–795.

Hanson, P., McRoberts, R., Isebrands, J., Dixon, R., 1987. An optimal sampling strategy for determining CO2 exchange rate as a function of photosynthetic photon flux density. Photosynthetica 21, 98–101.

Harlow, B.A., Marshall, J.D., Robinson, A.P., 2006. A multi-species comparison of $\delta^{13}C$ from whole wood, extractive-free wood and holocellulose. Tree Physiology 26, 767–774.

Holmes, R.L., 1983. Computer-assisted quality control in tree-ring dating and measurement. Tree-ring Bulletin 43, 69–78.

Hubbard, R.M., Bond, B.J., Ryan, M.G., 1999. Evidence that hydraulic conductance limits photosynthesis in old *Pinus ponderosa* trees. Tree Physiology 19, 165–172.

Jarvis, P.G., 1976. The interpretation of the variations in leaf water potential and stomatal conductance found in canopies in the field. Philosophical Transactions of the Royal Society of London. B, Biological Sciences 273, 593–610.

Johnsen, K., Samuelson, L., Teskey, R., McNulty, S., Fox, T., 2001. Process models as tools in forestry research and management. Forest Science 47, 2–8.

Koch, G.W., Sillett, S.C., Jennings, G.M., Davis, S.D., 2004. The limits to tree height. Nature 428, 851–854.

Korzukhin, M.D., Ter-Mikaelian, M.T., Wagner, R.G., 1996. Process versus empirical models: which approach for forest ecosystem management? Canadian Journal of Forest Research 26, 879–887.

Landsberg, J.J., Sands, P.J., 2011. Physiological Ecology of Forest Production: Principles, Processes and Models. Academic Press/Elsevier, Amsterdam, Boston.

Landsberg, J.J., Waring, R.H., 1997. A generalised model of forest productivity using simplified concepts of radiation-use efficiency, carbon balance and partitioning. Forest Ecology and Management 95, 209–228.

Landsberg, J.J., Waring, R.H., Coops, N.C., 2003. Performance of the forest productivity model 3-PG applied to a wide range of forest types. Forest Ecology and Management 172, 199–214.

Law, B.E., Ryan, M.G., Anthoni, P.M., 1999. Seasonal and annual respiration of a ponderosa pine ecosystem. Global Change Biology 5, 169–182.

Law, B.E., Waring, R.H., Anthoni, P.M., Aber, J.D., 2000. Measurements of gross and net ecosystem productivity and water vapour exchange of a *Pinus ponderosa* ecosystem, and an evaluation of two generalized models. Global Change Biology 6, 155–168.

Law, B.E., Goldstein, A.H., Anthoni, P.M., Unsworth, M.H., Panek, J.A., Bauer, M.R., Fracheboud, J.M., Hultman, N., 2001. Carbon dioxide and water vapor exchange by young and old ponderosa pine ecosystems during a dry summer. Tree Physiology 21, 299–308.

Mäkelä, A., Landsberg, J., Ek, A.R., Burk, T.E., Ter-Mikaelian, M., Ågren, G.I., Oliver, C.D., Puttonen, P., 2000. Process-based models for forest ecosystem management: current state of the art and challenges for practical implementation. Tree Physiology 20, 289–298.

McDowell, N.G., Phillips, N., Lunch, C., Bond, B.J., Ryan, M.G., 2002. An investigation of hydraulic limitation and compensation in large, old Douglas-fir trees. Tree Physiology 22, 763–774.

McFarlane, K.J., Schoenholtz, S.H., Powers, R.F., 2009. Plantation management intensity affects belowground carbon and nitrogen storage in Northern California. Soil Science Society of America Journal 73, 1020–1032.

McFarlane, K.J., Schoenholtz, S.H., Powers, R.F., Perakis, S.S., 2010. Soil organic matter stability in intensively managed ponderosa pine stands in California. Soil Science Society of America Journal 74, 979–992.

Nippert, J.B., Marshall, J.D., 2003. Sources of variation in ecophysiological parameters in Douglas-fir and grand fir canopies. Tree Physiology 23, 591–601.

Oliver, W.W., Powers, R.F., 1978. Growth Models for Ponderosa Pine: Yield of Unthinned Plantations in Northern California. Pacific Southwest Forest and Range Experiment Station, Forest Service, US Department of Agriculture.

Oliver, W.W., Ryker, R.A., 1990. Silvics of ponderosa pine. In: Burns, R.M., Honkala, B.H. (Eds.), Silvics of North America, vol. 1. Conifers. USDA Forest Services. pp. 413–424.

Paul, K.I., Booth, T.H., Jovanovic, T., Sands, P.J., Morris, J.D., 2007. Calibration of the forest growth model 3-PG to eucalypt plantations growing in low rainfall regions of Australia. Forest Ecology and Management 243, 237–247.

Pierce, L.L., Running, S.W., 1988. Rapid estimation of coniferous forest leaf area index using a portable integrating radiometer. Ecology, 1762–1767.

Powers, R.F., Ferrell, G.T., 1996. Moisture, nutrient, and insect constraints on plantation growth: the "Garden of Eden" experiment. New Zealand Journal of Forest Science 26 (1/2), 126–144.

Powers, R.F., Reynolds, P.E., 1999. Ten-year responses of ponderosa pine plantations to repeated vegetation and nutrient control along an environmental gradient. Canadian Journal of Forest Research 29, 1027–1038.

Powers, R.F., Ferrell, G.T., Koerber, T.W., 1992. The garden of Eden experiment: four-year growth of ponderosa pine plantations. In: Proceedings, Thirteenth Annual Forest Vegetation Management Conference. Forest Vegetation Management Conf., Redding, CA, Eureka, CA, pp. 46–63.

Powers, E.M., Marshall, J.D., Zhang, J., Wei, L., 2013. Post-fire management regimes affect carbon sequestration and storage in a Sierra Nevada mixed conifer forest. Forest Ecology and Management 291, 268–277.

Reynolds, P.E., Powers, R.F., Mitchell, A., Puttonen, P., Stoehr, M., Hawkins, B., 2000. Gas exchange for managed ponderosa pine stands positioned along a climatic gradient. Journal of Sustainable Forestry 10, 257–266.

Riegel, G.M., Miller, R.F., Krueger, W.C., 1992. Competition for resources between understory vegetation and overstory *Pinus ponderosa* in northeastern Oregon. Ecological Applications, 71–85.

Ryan, M.G., Yoder, B.J., 1997. Hydraulic limits to tree height and tree growth. BioScience 47, 235–242.

Ryan, M.G., Bond, B.J., Law, B.E., Hubbard, R.M., Woodruff, D., Cienciala, E., Kucera, J., 2000. Transpiration and whole-tree conductance in ponderosa pine trees of different heights. Oecologia 124, 553–560.

Sands, P.J., 2001. 3PGpjs-a User-friendly Interface to 3-PG, The Landsberg and Waring Model of Forest Productivity. Technical Report No. 29, Edition 2. CRC for Sustainable Production Forestry and CSIRO Forestry and Forest Products, Hobart, Australia, p. 25.

Sands, P.J., Landsberg, J.J., 2002. Parameterisation of 3-PG for plantation grown *Eucalyptus globulus*. Forest Ecology and Management 163, 273–292.

Shainsky, L.J., Radosevich, S.R., 1986. Growth and water relations of *Pinus Ponderosa* seedlings in competitive regimes with *Arctostaphylos patula* seedlings. Journal of Applied Ecology 23, 957–966.

Swenson, J.J., Waring, R.H., Fan, W., Coops, N., 2005. Predicting site index with a physiologically based growth model across Oregon, USA. Canadian Journal of Forest Research 35, 1697–1707.

Ubierna, N., Marshall, J.D., 2011. Estimation of canopy average mesophyll conductance using $\delta^{13}C$ of phloem contents. Plant, Cell & Environment 34, 1521–1535.

Uddling, J., Hall, M., Wallin, G., Karlsson, P.E., 2005. Measuring and modelling stomatal conductance and photosynthesis in mature birch in Sweden. Agricultural and Forest Meteorology 132, 115–131.

Van Pelt, R., Franklin, J.F., 2000. Influence of canopy structure on the understory environment in tall, old-growth, conifer forests. Canadian Journal of Forest Research 30, 1231–1245.

Waring, R.H., Landsberg, J.J., Williams, M., 1998. Net primary production of forests: a constant fraction of gross primary production? Tree Physiology 18, 129–134.

Wei, L., Marshall, J.D., Link, T.E., Kavanagh, K.L., Du, E., Pangle, R.E., Gag, P.J., Ubierna, N., 2014. Constraining 3-PG with a new $\delta^{13}C$ sub-model: a test using the $\delta^{13}C$ of tree rings. Plant, Cell & Environment,. http://dx.doi.org/10.1111/pce.12133.

Whitehead, D., Hall, G., Walcroft, A., Brown, K., Landsberg, J., Tissue, D., Turnbull, M., Griffin, K., Schuster, W., Carswell, F., Trotter, C., James, I., Norton, D., 2002. Analysis of the growth of rimu (*Dacrydium cupressinum*) in South Westland, New Zealand, using process-based simulation models. International Journal of Biometeorology 46, 66–75.

Wykoff, W.R., Crookston, N.L., Stage, A.R., 1982. User's guide to the stand prognosis model. In: USDA Forest Service, Intermountain Forest and Range Experiment Station, p. 112.

Xenakis, G., Ray, D., Mencuccini, M., 2008. Sensitivity and uncertainty analysis from a coupled 3-PG and soil organic matter decomposition model. Ecological Modelling 219, 1–16.

Xu, M., DeBiase, T.A., Qi, Y., Goldstein, A., Liu, Z., 2001. Ecosystem respiration in a young ponderosa pine plantation in the Sierra Nevada Mountains, California. Tree Physiology 21, 309–318.

Zhang, J., Marshall, J.D., Fins, L., 1996. Correlated population differences in dry matter accumulation, allocation, and water-use efficiency in three sympatric conifer species. Forest Science 42, 242–249.

Zhang, J., Powers, R.F., Skinner, C.N., 2010. To manage or not to manage: the role of silviculture in sequestering carbon in the specter of climate change. In: USDA Forest Service Proceedings, RMRS P-61.

Zhang, J., Powers, R.F., Oliver, W.W., Young, D.H., 2013. Response of ponderosa pine plantations to competing vegetation control in Northern California, USA: a meta-analysis. Forestry, 3–11.